# QUINTESSENCE

ARTUR ALHO, <sup>1\*</sup> ELSA BERNHOLM, <sup>2†</sup> AND CLAES UGGLA, <sup>2‡</sup>
<sup>1</sup> Center for Mathematical Analysis, Geometry and Dynamical Systems,
Instituto Superior Técnico, Universidade de Lisboa,
Av. Rovisco Pais, 1049-001 Lisboa, Portugal.

<sup>2</sup> Department of Physics, Karlstad University,
S-65188 Karlstad, Sweden.

#### Abstract

Recent observations suggest that the accelerated expansion of the Universe at late times is caused by a temporally changing dark energy component, rather than the constant one in the standard  $\Lambda$ CDM scenario. In this context quintessence, i.e. a canonical scalar field minimally coupled to gravity, plays a prominent role. There are, however, three main types of quintessence models: thawing quintessence, scaling freezing quintessence, and tracking quintessence. Dynamical systems reformulations of the field equations for a broad set of scalar field potentials, including some new ones, allow us to use dynamical systems methods to derive global and asymptotic features, visualised in bounded state space pictures clearly illustrating the relationships and properties of the different types of quintessence, clarifying initial data issues, and yielding simple and accurate approximations.

Keywords: General Relativity, Quintessence, dynamical systems.

#### 1 Introduction

Within the interpretative context of General Relativity (GR), increasingly precise cosmological observations suggest that (i) the Universe is almost spatially homogeneous, isotropic and flat on large spatial scales, (ii) it undergoes a late phase of accelerated expansion requiring a 'dark energy' (DE) density component,  $\rho_{\rm DE} > 0$ , with a pressure  $p_{\rm DE} < -\rho_{\rm DE}/3$ , (iii) most of the matter in the Universe is invisible 'cold dark matter' (CDM) without pressure.

The simplest model that is compatible with these features is the  $\Lambda$ CDM model, for which  $\rho_{\rm DE} = -p_{\rm DE} = \Lambda > 0$ , where  $\Lambda$  is the cosmological constant. However,  $\rho_{\rm DE}$  might be dynamical, as suggested by some recent cosmological observations. One of the simplest and theoretically most appealing dynamical DE models is a canonical scalar field,  $\varphi$ , minimally coupled to gravity, referred to as quintessence, the fifth element of the current matter content in the Universe after radiation, neutrinos, baryons and dark matter.

Different spatially homogeneous, isotropic and flat GR quintessence models, denoted by  $\varphi$ CDM, are characterised by the scalar field potential  $V(\varphi)$  and the evolution of the equation of state parameter  $w_{\rm DE} = w_{\varphi} \equiv p_{\varphi}/\rho_{\varphi}$ . For brevity and simplicity we in this paper only consider monotonically decreasing potentials  $V(\varphi) > 0$ ,

$$\lambda \equiv -\frac{d\ln V}{d\varphi} > 0,\tag{1}$$

<sup>\*</sup>Electronic address:aalho@math.ist.utl.pt

<sup>†</sup>Electronic address:elsabernholm@gmail.com

<sup>&</sup>lt;sup>‡</sup>Electronic address:claes.uggla@kau.se

1 INTRODUCTION 2

and matter consisting of baryons and CDM, i.e., matter is modelled as a pressure-free fluid with energy density  $\rho_{\rm m} > 0$ . Most  $\varphi$ CDM solutions are not cosmologically relevant. However, certain particular quintessence 'attractor' solutions are of cosmological interest; moreover, they attract and thereby approximate open sets of other viable solutions, from the matter-dominated epoch to the asymptotic future.

Quintessence evolution is conveniently described by thawing,  $w_{\varphi} \approx -1$ ,  $dw_{\varphi}/da > 0$ , and freezing,  $w_{\varphi} > -1$ ,  $dw_{\varphi}/da < 0$ , where a is the cosmological scale factor [1]. There are, however, quintessence models that go through several periods of both thawing and freezing. To obtain an unambiguous nomenclature we consider the past asymptotic features of  $w_{\varphi}$  and  $\lambda(\varphi)$  for the attractor solutions, which lead to three main types of quintessence:

- (I) All  $\varphi$ CDM models admit thawing quintessence attractor solutions, parameterised by  $\lim_{a\to 0} \varphi = \varphi_*$  (and thereby  $\lim_{a\to 0} \lambda = \lambda(\varphi_*) \equiv \lambda_*$ ) and  $w_\infty \equiv \lim_{a\to 0} w_\varphi = -1$ .
- (II) Models with  $\lambda_{-} = \lim_{a\to 0} \lambda \gg 1$  and  $w_{\infty} = 0$  admit a single scaling freezing quintessence attractor solution with an initial matter-dominated epoch,  $\lim_{a\to 0} (\rho_{\varphi}/\rho_{\rm m}) \ll 1$ .
- (III) Models that satisfy  $\lim_{\varphi \to 0} \varphi^{1+r} \lambda(\varphi) = p > 0$ ,  $r \ge 0$  (r = 0 (r > 0) corresponds to asymptotically (exponentially) inverse power-law potentials), admit a single tracking quintessence attractor solution with  $-1 < w_{\infty} = -2/(2+p) < 0$  when r = 0 and  $w_{\infty} = 0$  when r > 0.

The field equations for the  $\varphi$ CDM models are the Friedmann and Raychaudhuri equations, the non-linear Klein-Gordon equation, and the matter conservation equation:

$$3H^2 = \rho,\tag{2a}$$

$$\dot{H} + H^2 = -\frac{1}{6}(\rho + 3p),$$
 (2b)

$$\ddot{\varphi} = -3H\dot{\varphi} - V_{.\varphi},\tag{2c}$$

$$\dot{\rho}_{\rm m} = -3H\rho_{\rm m},\tag{2d}$$

where an overdot represents the derivative with respect to the cosmic proper time t whereas the Hubble scalar is defined by  $H = \dot{a}/a$ ; the total energy density  $\rho$  and pressure p are given by

$$\rho = \rho_{\varphi} + \rho_{\rm m}, \qquad p = p_{\varphi}, \tag{3}$$

where

$$\rho_{\varphi} = \frac{1}{2}\dot{\varphi}^2 + V(\varphi), \qquad p_{\varphi} = \frac{1}{2}\dot{\varphi}^2 - V(\varphi). \tag{4}$$

Since  $\rho > 0$  it follows from (2a) that H(t) > 0 for initially expanding models. By introducing  $\dot{\varphi}$  as a variable the above equations form a four-dimensional (4D) dynamical system<sup>2</sup> for the state vector  $(H, \varphi, \dot{\varphi}, \rho_{\rm m})$  obeying the constraint (2a).

In the next two sections we introduce dimensionless variables and 3D unconstrained regular dynamical systems, yielding state space pictures that show that the scaling freezing and tracking quintessence attractor solutions, respectively, form the interior state space boundary of one-parameter sets of thawing quintessence solutions. Section 4 introduces quintessence approximations that are simpler and more accurate than earlier ones in the literature. Finally, Section 5 discusses dynamical systems formulations and features for generalisations of the present illustrative examples and for other types of scalar field potentials, and it also provides references outlining the history of scalar field cosmology.

 $<sup>^{1}</sup>$ The name tracking quintessence is also sometimes used in the literature for scaling freezing quintessence, due to that in both cases there is an open set of solutions that track, i.e. shadow, a single 'attractor' solution.

<sup>&</sup>lt;sup>2</sup>A (continuous) dynamical system is a set of autonomous first order ordinary differential equations  $\dot{\mathbf{x}} = \mathbf{f}(\mathbf{x})$ ,  $\mathbf{x} \subseteq \mathbb{R}^n$ . A regular dynamical system requires that  $\mathbf{f}(\mathbf{x})$  is at least  $C^1$ -differentiable, which enables a local eigenvalue analysis at fixed points (also known as critical points, equilibrium points)  $\mathbf{x}_0$ ,  $\mathbf{f}(\mathbf{x}_0) = 0$ .

### 2 Thawing and scaling freezing quintessence

We begin by introducing some physically interesting dimensionless Hubble-normalised quantities: the Hubble-normalised matter and scalar field energy densities, where the latter consists of the Hubble-normalised kinetic and potential parts,

$$\Omega_{\rm m} \equiv \frac{\rho_{\rm m}}{3H^2}, \qquad \Omega_{\varphi} \equiv \frac{\rho_{\varphi}}{3H^2} = \Omega_T + \Omega_V, \qquad \Omega_T \equiv \frac{\dot{\varphi}^2}{6H^2}, \qquad \Omega_V \equiv \frac{V(\varphi)}{3H^2}.$$
(5)

It follows that (2a) then yields

$$\Omega_{\varphi} + \Omega_{\rm m} = \Omega_T + \Omega_V + \Omega_{\rm m} = 1, \tag{6}$$

wheras (4) results in

$$w_{\varphi} \equiv \frac{p_{\varphi}}{\rho_{\varphi}} = \frac{\Omega_T - \Omega_V}{\Omega_T + \Omega_V} = -1 + \frac{2\Omega_T}{\Omega_T + \Omega_V} \in [-1, 1], \tag{7}$$

where  $w_{\varphi} = -1$  when  $\dot{\varphi} = 0$ ,  $\Omega_T = 0$ ,  $\Omega_V > 0$ , while  $w_{\varphi} = 1$  when V = 0,  $\Omega_V = 0$ ,  $\Omega_T > 0$ . As follows from (2a) and (2b), the deceleration parameter q is given by

$$q \equiv -\frac{a\ddot{a}}{\dot{a}^2} = -\left(1 + \frac{H'}{H}\right) = \frac{1}{2}\left(1 + 3w_{\varphi}\Omega_{\varphi}\right) = \frac{1}{2}\left[1 + 3\left(\Omega_T - \Omega_V\right)\right] \in [-1, 2],\tag{8}$$

where a ' henceforth denotes the derivative with respect to the e-fold time

$$N \equiv \ln(a/a_0), \qquad a_0 = a(t_0), \tag{9}$$

where  $t_0$  is some reference time, from which it follows that dN/dt = H and  $a \to 0 \Rightarrow N \to -\infty$ ; q = -1 when  $w_{\varphi} = -1$  and  $\Omega_T = 0$ ,  $\Omega_V = 1$  while q = 2 when  $w_{\varphi} = 1$  and  $\Omega_T = 1$ ,  $\Omega_V = 0$ .

Next we follow [2] (AUW1) and introduce

$$u \equiv \frac{\dot{\varphi}}{\sqrt{\rho_{\varphi}}} = \frac{\varphi'}{\sqrt{3\Omega_{\varphi}}}, \qquad v \equiv \sqrt{\frac{\Omega_{\varphi}}{3}},$$
 (10)

which leads to

$$w_{\varphi} = u^2 - 1, \qquad \Omega_{\rm m} = 1 - 3v^2, \qquad \Omega_{\varphi} = 3v^2,$$
 (11a)

$$\Omega_T = \frac{3}{2} (uv)^2, \qquad \Omega_V = \frac{3}{2} (2 - u^2) v^2, \qquad q = \frac{1}{2} (1 + 9(u^2 - 1)v^2), \qquad (11b)$$

and thus

$$u \in [-\sqrt{2}, \sqrt{2}], \qquad v \in [0, 1/\sqrt{3}],$$
 (12)

where u = const.; w = const.; v = const.; v = const., with boundary values  $u = \pm\sqrt{2} \Rightarrow w_{\varphi} = 1$ ,  $\Omega_V = 0$ ;  $v = 0 \Rightarrow \Omega_{\varphi} = 0$ ,  $\Omega_{\text{m}} = 1$ ;  $v = 1/\sqrt{3} \Rightarrow \Omega_{\varphi} = 1$ ,  $\Omega_{\text{m}} = 0$ .

The variables u and v are appropriate for models with bounded  $\lambda(\varphi)$  and  $\lim_{\varphi \to \pm \infty} \lambda(\varphi) = \lambda_{\pm} = \text{const.}$ , but in order to obtain a bounded state space, which is a desirable property both for mathematical and illustrative purposes, we also need to introduce a bounded variable monotonically increasing in  $\varphi$ ,  $\bar{\varphi} \in [\bar{\varphi}_{-}, \bar{\varphi}_{+}]$ , where we for simplicity require  $\bar{\varphi}_{\pm} \equiv \lim_{\varphi \to \pm \infty} \bar{\varphi} = \pm 1$ . This leads to the following dynamical system<sup>3</sup>

$$\bar{\varphi}' = 3uvG(\bar{\varphi}),\tag{13a}$$

$$u' = \frac{3}{2}(2 - u^2)(v\lambda(\bar{\varphi}) - u),$$
 (13b)

$$v' = \frac{3}{2}(1 - u^2)(1 - 3v^2)v,$$
(13c)

<sup>&</sup>lt;sup>3</sup>Using  $w_{\varphi}$  and  $\Omega_{\varphi}$  instead of u and v lead to a non-regular dynamical system.

where

$$G(\bar{\varphi}) \equiv \left(\frac{d\bar{\varphi}}{d\varphi}\right) > 0, \quad \bar{\varphi} \in (-1,1); \qquad G(\pm 1) = 0.$$
 (14)

For a wide class of potentials  $V(\varphi)$ ,  $\bar{\varphi}(\varphi)$  can be adapted to the properties of  $\lambda(\varphi)$  so that both  $G(\bar{\varphi})$  and, with a slight abuse of notation,  $\lambda(\bar{\varphi})$  are regular functions and  $\lambda(\bar{\varphi})$  has limits  $\lambda_{\pm} = \lambda(\pm 1), \ \lambda_{-} \geq \lambda_{+} \geq 0$ , where  $\lambda_{+} = \lambda_{-} \Rightarrow \lambda = \text{constant} = \lambda_{+} = \lambda_{-}$ , which yields  $V = V_{*} \exp(-\lambda \varphi)$ . Eq. (13) then forms an unconstrained regular dynamical system on a 3D 'box state space'  $(\bar{\varphi}, u, v)$  bounded by 2D invariant boundary sets.

The equations are easily solved on the boundaries v=0 and  $u=\pm\sqrt{2}$  where the solutions are independent of  $\lambda(\bar{\varphi})$  and  $V(\varphi)$ : On the matter-dominated Friedmann-Lemaître boundary v=0 ( $\Omega_{\rm m}=1$ ) there are three lines of fixed points,  ${\rm FL}_0^{\varphi_*}$ , with u=0 ( $w_{\varphi}=-1$ ) and  ${\rm FL}_{\pm}^{\varphi_*}$ , with  $u=\pm\sqrt{2}$  ( $w_{\varphi}=1$ ), connected by the solutions  ${\rm FL}_{\pm}^{\varphi_*}\to {\rm FL}_0^{\varphi_*}$  with  $\bar{\varphi}=\bar{\varphi}_*={\rm const.}$ ; on  $u=\pm\sqrt{2}$  the solutions originate from the 'kinaton' fixed points  ${\rm K}_{\pm}^{\mp}$  ( $\Omega_T=1$ ) where each solution end at a distinct fixed point on  ${\rm FL}_{\pm}^{\varphi_*}$ , see Figure 1(a).

It follows from (13a) that  $\bar{\varphi}(N) \in (-1,1)$  is monotonically increasing (decreasing) when v>0 and u>0 (u<0). For monotonically decreasing potentials,  $\lambda(\bar{\varphi})>0$ ,  $\bar{\varphi}\in (-1,1)$ , it follows from (13b) that all 'interior' solutions reach the region u>0, since u is monotonically increasing when v>0 and  $u\leq 0$ . Moreover,  $3H^2=2V(\bar{\varphi})/3(2-u^2)v^2$  is a monotonic function, which prevents fixed points and recurring orbits when v>0 and  $\bar{\varphi}\in (-1,1)$ , and hence all such solutions originate and end at the boundaries v=0 or  $\bar{\varphi}=\pm 1$ . In addition, the equations on  $\bar{\varphi}=\pm 1$  form the same coupled system of equations for (u,v) as when  $V=V_*\exp(-\lambda_{\pm}\varphi)$ . When all this is taken together with the known solution structure on the boundaries, it follows that all solutions for the present class of models originate and end at different fixed points residing on the boundaries v=0 and  $\bar{\varphi}=\pm 1$ .

The line of fixed points  $\mathrm{FL}_0^{\varphi_*}$  is central for thawing quintessence. Linearisation of (13) at  $\mathrm{FL}_0^{\varphi_*}$ , where  $w_{\varphi}=-1$ , results in that at each fixed point on  $\mathrm{FL}_0^{\varphi_*}$  there is

- (i) a zero eigenvalue  $\Rightarrow$  the line of fixed points  $FL_0^{\varphi_*}$ ;
- (ii) a negative eigenvalue  $\Rightarrow$  the solutions  $FL_{\pm}^{\varphi_*} \to FL_0^{\varphi_*}$  on v = 0 ( $\Omega_m = 1$ ), with 'frozen' scalar field values  $\bar{\varphi} = \bar{\varphi}_* = \text{const.}$ , constituting the stable manifold of  $FL_0^{\varphi_*}$ ;
- (iii) a positive eigenvalue  $\Rightarrow$  a single solution originating from each fixed point on  $\mathrm{FL}_0^{\varphi_*}$  with an eigenvector with u > 0, except for the  $\Lambda\mathrm{CDM}$  case with  $\lambda = 0$ , see the Figures below. Taken together, these solutions form the 2D unstable manifold surface of solutions of  $\mathrm{FL}_0^{\varphi_*}$ .

The observational requirement of a long matter-dominated epoch,  $\Omega_{\rm m} \approx 1 \ (v \approx 0)$ , poses severe restrictions on viable initial data. For monotonically decreasing potentials generic solutions originate from fixed points on the kinaton boundary  $\Omega_T = 1$ . It is only a 'small' open set of these solutions that is relevant for thawing quintessence, since a long matter-dominated epoch requires thawing quintessence solutions to come very close to the matter-dominated v = 0 boundary. There these solution closely shadow the solutions  ${\rm FL}_{\pm}^{\varphi_*} \to {\rm FL}_0^{\varphi_*}$  and are thereby pushed to the 'attractor' solutions on the unstable manifold of  ${\rm FL}_0^{\varphi_*}$ , which hence approximate them extremely well during their observationally relevant evolution — this is the thawing quintessence 'attractor' mechanism (together with, as we will see, the existence of a common fixed point as the sink and true future attractor). Finally, note that  $\varphi$  acts as a frozen test field that does not affect the spacetime geometry during the matter-dominated epoch, where u(N) (and thereby  $w_{\varphi}(N)$ ) does not describe anything observable.

As an illustration, consider first  $V = V_* \exp(-\lambda \varphi)$  for which the equation for  $\bar{\varphi}$  decouples, resulting in a 2D reduced dynamical system of coupled equations for u and v. However, we also consider  $\bar{\varphi}$  in order to make comparisons since all other potentials yield non-trivial  $\lambda(\bar{\varphi})$  and 3D coupled systems of equations; a simple choice of  $\bar{\varphi}$  is  $\bar{\varphi} \equiv \tanh(\varphi) \Rightarrow G(\bar{\varphi}) = 1 - \bar{\varphi}^2$ ,  $\bar{\varphi} \in [-1, 1]$ .

Due to the decoupling of  $\bar{\varphi}$ , projecting solutions with  $\bar{\varphi} \in (-1,1)$  onto the (u,v)-plane results in the same trajectories as those on the boundaries  $\bar{\varphi} = \pm 1$ .

When  $V=\Lambda>0 \Rightarrow \lambda=0$ , the unstable manifold of  $\mathrm{FL}_0^{\varphi_*}$ , referred to as  $\mathrm{UFL}_0^{\varphi_*}$ , is given by the  $\Lambda\mathrm{CDM}$  solutions  $\mathrm{FL}_0^{\varphi_*}\to\mathrm{dS}^{\varphi_*}$  on the, in this case, invariant u=0 subset, see eq. (13b), with  $\bar{\varphi}=\bar{\varphi}_*=\mathrm{const.}$ , where dS stands for de Sitter. Increasing  $\lambda$  results in increasing deformations of the  $\mathrm{UFL}_0^{\varphi_*}$  surface of solutions. When  $\lambda>\sqrt{3}$  the solution  $\mathrm{S}^-\to\mathrm{S}^+$ , with  $(u,v)=(1,1/\lambda)$  and thereby  $w_\varphi=0$ ,  $\Omega_\varphi=3/\lambda^2$ , replaces  $\mathrm{P}^-\to\mathrm{P}^+$ , with  $(u,v)=(\lambda,1)/\sqrt{3}$ , as the  $\bar{\varphi}\in(-1,1)$ -boundary of the  $\mathrm{UFL}_0^{\varphi_*}$  surface of solutions (where  $\mathrm{P}^+$  (S<sup>+</sup>) is the future attractor when  $\lambda\leq\sqrt{3}$  ( $\lambda>\sqrt{3}$ )). See Figure 1 and AUW1 for further details.

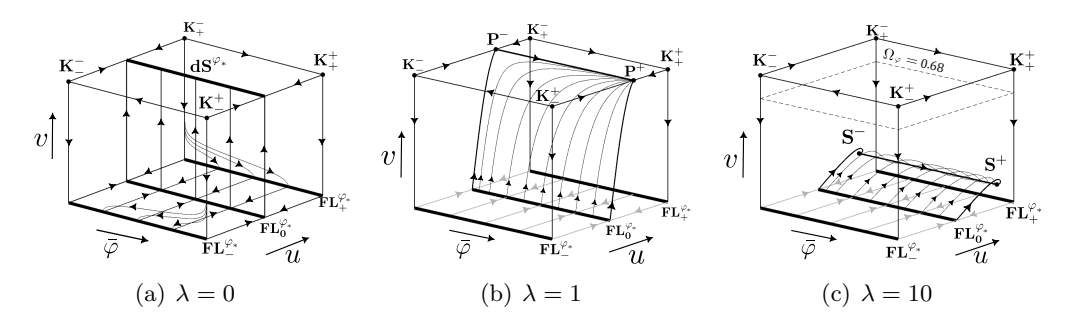


Figure 1: Solutions  $\operatorname{FL}_{\pm}^{\varphi_*} \to \operatorname{FL}_0^{\varphi_*}$  on the matter-dominated boundary v=0 ( $\Omega_{\mathrm{m}}=1$ ), which provide the thawing quintessence attractor mechanism, and solutions on the unstable  $\operatorname{FL}_0^{\varphi_*}$  manifold surface ( $\operatorname{UFL}_0^{\varphi_*}$ ) for  $V \propto \exp(-\lambda \varphi)$ . Figure (a) also depicts solutions  $\operatorname{K}_{\pm}^{\mp} \to \operatorname{FL}_{\pm}^{\varphi_*}$  on the boundaries  $u=\pm\sqrt{2}$  ( $\Omega_V=0$ ). Figure (b) illustrates that there are classes of potentials that continuously deform the  $\Lambda\operatorname{CDM}\operatorname{UFL}_0^{\varphi_*}$  with u=0 in Figure (a) to a thawing quintessence  $\operatorname{UFL}_0^{\varphi_*}$ . The boundary  $\operatorname{P}^- \to \operatorname{P}^+$  of  $\operatorname{UFL}_0^{\varphi_*}$  in Figure (b) is replaced with the scaling solution  $\operatorname{S}^- \to \operatorname{S}^+$  in Figure (c) when  $\lambda > \sqrt{3}$ , where the scaling matter-dominant condition  $\lambda \gg 1$  implies that  $\Omega_{\varphi}$  never becomes observationally significant for either type of quintessence.

Next we consider scaling freezing quintessence, which requires potentials with varying  $\lambda(\bar{\varphi})$ , where early matter-domination and future eternal accelerated expansion demands  $\lambda_{-} \gg 1$ ,  $0 \leq \lambda_{+} \lesssim \mathcal{O}(1)$ , respectively. Following AUW1, we illustrate the relationship between scaling freezing and thawing quintessence with the potential

$$V = M_{-}^{4} e^{-\lambda_{-}\varphi} + M_{+}^{4} e^{-\lambda_{+}\varphi}, \qquad M_{\pm} > 0, \qquad \lambda_{-} > \lambda_{+} \ge 0,$$
 (15)

where we choose

$$\bar{\varphi} = \tanh(C\varphi + D), \qquad C = \frac{1}{2}(\lambda_{-} - \lambda_{+}), \qquad D = \ln[(M_{+}/M_{-})^{4}],$$
 (16)

which leads to

$$\lambda(\bar{\varphi}) = \frac{1}{2}\lambda_{+}(1+\bar{\varphi}) + \frac{1}{2}\lambda_{-}(1-\bar{\varphi}), \qquad G(\bar{\varphi}) = C(1-\varphi^{2}). \tag{17}$$

As seen in Figure 2(a), the thawing quintessence  $\mathbf{UFL}_0^{\varphi_*}$  surface can be viewed as a continuous deformation in u and v of its boundary solutions  $\mathrm{FL}_0^{\varphi_*} \to \mathrm{S}^-$  and  $\mathrm{FL}_0^{\varphi_*} \to \mathrm{P}^+$  (dS<sup>+</sup> if  $\lambda_+ = 0$ ) on  $\bar{\varphi} = \pm 1$ , while the scaling freezing solution  $\mathrm{S}^- \to \mathrm{P}^+$  forms the interior boundary of  $\mathbf{UFL}_0^{\varphi_*}$ , describing the late evolution of thawing quintessence. By choosing  $\lambda_\pm$  appropriately both the scaling freezing and thawing solutions become observationally viable. The scaling

<sup>&</sup>lt;sup>4</sup>The kernel P stands for Power-law since  $0 < \lambda < \sqrt{2}$  yields power-law accelerated expansion. The kernel S denotes Scaling, since  $v = 1/\lambda \Rightarrow \rho_{\varphi}(N)/\rho_{\rm m}(N) = \Omega_{\varphi}/\Omega_{\rm m} = \Omega_{\varphi}/(1-\Omega_{\varphi}) = 3v^2/(1-3v^2) = 3/(\lambda^2-3)$ , and hence  $\rho_{\rm m}(N) \propto \exp(-3N) \propto a^{-3}$  and  $\rho_{\varphi}(N)$  'scale' in the same manner (are proportional).

freezing quintessence attractor mechanism is due to that the  $\bar{\varphi}=-1$  boundary is the stable manifold of S<sup>-</sup>, while the scaling freezing solution is its unstable manifold. A long matter-dominated scaling epoch requires initial data to be extremely close to S<sup>-</sup> with  $\bar{\varphi}\approx-1$ , where the vicinity to the stable manifold of S<sup>-</sup> pushes an open set of solutions toward the solution S<sup>-</sup>  $\rightarrow$  P<sup>+</sup> near S<sup>-</sup>, where S<sup>-</sup>  $\rightarrow$  P<sup>+</sup> is subsequently shadowed and thereby approximate these solutions extremely well, a phenomenon further strengthened by that P<sup>+</sup>/dS<sup>+</sup> is the true future attractor where all interior solutions end.

The next example is the following inflationary  $\alpha$ -attractor quintessence potential, introduced in [3] and studied from a dynamical systems perspective in [4], although we here omit radiation:

$$V = V_* \left( \frac{e^{-\nu(1+\bar{\varphi})} - e^{-2\nu}}{1 - e^{-2\nu}} \right), \qquad \bar{\varphi} \equiv \tanh \frac{\varphi}{\sqrt{6\alpha}}, \qquad \lambda = \frac{\nu}{\sqrt{6\alpha}} \left( \frac{1 - \bar{\varphi}^2}{1 - e^{-\nu(1-\bar{\varphi})}} \right). \tag{18}$$

Inflationary  $\alpha$ -attractor arguments suggest that  $\alpha \sim \mathcal{O}(1)$  while inflationary and quintessence energy considerations result in large values for  $V_*$ ,  $\varphi_*$  and  $\nu \sim \mathcal{O}(125)$ , see [5]. We choose  $\alpha = 7/3$  and, for illustrative purposes,  $\nu = 15$ .

Figure 2(b) depicts the inflationary attractor solution  $dS^- \to P^+$  on the scalar field boundary  $v = 1/\sqrt{3}$  ( $\Omega_{\varphi} = 1$ ) and thawing attractor solutions on  $UFL_0^{\varphi_*}$ . The inflationary attractor solution is the unstable centre manifold of the fixed point  $dS^-$ , corresponding to an eigenvalue that is zero, while  $dS^-$  is a sink on the  $\bar{\varphi} = -1$  boundary associated with two negative eigenvalues. This latter feature pushes nearby solutions toward the inflationary attractor solution where the zero eigenvalue strengthens its attracting nature and also enables solutions to stay in a long inflationary quasi-de Sitter epoch in the vicinity of  $dS^-$ . Figure 2(b) also illustrates that the inflationary attractor solution goes through a 'kinaton' epoch ( $\Omega_T \approx 1$ ) when it shadows the kinaton solution  $K_+^- \to K_+^+$ , a feature that is enhanced with increasing  $\nu$ , see [4]. Note that  $\nu$  ( $\Omega_{\varphi}$ ) is monotonically decreasing when  $\nu$  is enhanced with  $\bar{\varphi}_* \approx 1$  (corresponding to values  $\varphi_*$  on the exponential tail of the potential where  $\lambda(\varphi_*) \lesssim \mathcal{O}(1)$ ) that are observationally viable.

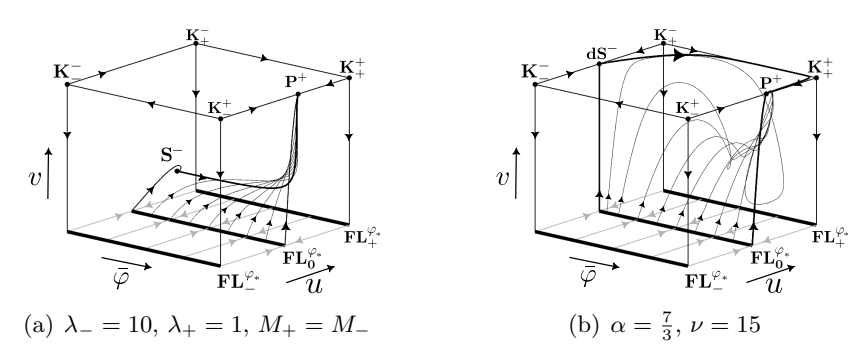


Figure 2: (a) Depicts the surface of thawing quintessence attractor solutions with the scaling freezing attractor solution  $S^- \to P^+$  as its interior boundary for the potential  $V = M_-^4 e^{-\lambda_- \varphi} + M_+^4 e^{-\lambda_+ \varphi}$ . (b) Depicts the inflationary  $\alpha$ -attractor solution for  $V \propto \frac{e^{-\nu(1+\tanh\frac{\varphi}{\sqrt{6}\alpha})} - e^{-2\nu}}{1-e^{-2\nu}}$  on the scalar field boundary  $v = 1/\sqrt{3}$  ( $\Omega_{\varphi} = 1$ ) and the surface of thawing quintessence attractor solutions, where only those with  $\bar{\varphi}_* \approx 1$  are cosmologically viable.

## 3 Thawing and tracking quintessence

The term tracking quintessence was introduced by Steinhardt et al. in [6, 7] for models with  $V \propto \varphi^{-p}$ , p > 0 and  $V \propto \exp(M/\varphi) - 1$ . In [8] (AUW2) the first case was generalised

to asymptotically inverse power-law potentials when  $\varphi \to 0$  and here we will also consider generalisations of the second case. In contrast to what was stated by Tsujikawa in the review [9], there are three types of tracking quintessence: tracking freezing, tracking constant and tracking thawing quintessence, as illustrated by the asymptotically inverse power-law potentials

$$V = V_* \left[ \frac{\nu(\cosh \nu \varphi)^{1-\alpha}}{\sinh(\nu \varphi)} \right]^p \tag{19}$$

discussed in AUW2. For brevity we here only consider  $\alpha = 1$ , i.e.,

$$V = V_* \sinh^{-p}(\nu \varphi), \quad p > 0, \quad \nu > 0 \quad \Rightarrow \quad \lambda = \frac{p\nu}{\tanh(\nu \varphi)} > 0.$$
 (20)

It follows that  $\lambda_+ = p\nu$ . We choose  $\bar{\varphi} = \tanh(\nu\varphi)$ ,  $\bar{\varphi} \in [0,1]$ . The previous variable v now results in that the equations become irregular at  $\bar{\varphi} = 0$  since  $\lim_{\bar{\varphi} \to 0} (\bar{\varphi}\lambda(\bar{\varphi})) = p$ .

Since u, which we keep, is bounded, so is  $v\lambda(\bar{\varphi})$  in eq. (13b). To regularise the equations we absorb the asymptotic factor in  $\lambda(\bar{\varphi})$  into v, leading to the following generalised definition of v:

$$v \equiv \bar{\varphi}^{-k} \sqrt{\frac{\Omega_{\varphi}}{3}},\tag{21}$$

where k=0 for the previous bounded  $\lambda$  models whereas we set k=1 for the present asymptotically inverse power-law potentials. Thus v becomes unbounded when  $\bar{\varphi} \to 0$ , leading to the 'ski-slope' state space in Figure 3 with two matter-dominated boundaries ( $\Omega_{\rm m}=1$ ), v=0,  $\bar{\varphi}=0$ , and the regular dynamical system,

$$\bar{\varphi}' = 3\nu\bar{\varphi}(1-\bar{\varphi}^2)\,uv,\tag{22a}$$

$$u' = \frac{3}{2}(2 - u^2)(p\nu \, v - u),\tag{22b}$$

$$v' = \frac{3}{2} \left[ (1 - u^2)(1 - 3\bar{\varphi}^2 v^2) - 2\nu(1 - \bar{\varphi}^2) uv \right] v.$$
 (22c)

Although v is unbounded all physical tracking quintessence features are in a bounded part of the state space: the matter-dominated tracker fixed point T, which is a spiral sink on the matter-dominated  $\bar{\varphi}=0$  boundary, is given by  $(\bar{\varphi},u,v)=u_{\rm T}(0,1,1/p\nu),\,u_{\rm T}=\sqrt{\frac{p}{2+p}}>0$ , which together with that u'>0 when  $u\leq 0$  ensures that the tracking quintessence attractor solution  $T\to P$ , the unstable manifold of T, is in a bounded part with u>0 of the interior state space, with  $P(\bar{\varphi},u,v)=(1,p\nu/\sqrt{3},1/\sqrt{3})$  being the future global attractor. The tracking quintessence attractor mechanism is similar to the scaling freezing attractor mechanism, i.e., an open set of solutions are pushed toward the 'attractor' solution  $T\to P$  near T by the unstable manifold of T (the  $\bar{\varphi}=0$  boundary set), resulting in that these solutions 'track', i.e. shadow,  $T\to P$ , which thereby approximate them extremely well during their observationally relevant evolution, and where, similarly to the scaling freezing case,  $T\to P$  is the interior boundary of  ${\rm UFL}_0^{\varphi*}$ .

We then note that

$$1 + w_{\varphi}|_{T} = u_{T}^{2} = \frac{p}{2+p}, \qquad 1 + w_{\varphi}|_{P} = u_{P}^{2} = \frac{1}{3}\lambda_{+}^{2} = \frac{1}{3}(p\nu)^{2},$$
 (23)

which results in three cases:

$$u_{\rm T} = \sqrt{\frac{p}{2+p}} > u_{\rm P} = p\nu/\sqrt{3} \quad \Rightarrow \quad \nu < \sqrt{\frac{3}{p(2+p)}},$$
 (24a)

$$u_{\rm T} = \sqrt{\frac{p}{2+p}} = u_{\rm P} = p\nu/\sqrt{3} \quad \Rightarrow \quad \nu = \sqrt{\frac{3}{p(2+p)}},$$
 (24b)

$$u_{\rm T} = \sqrt{\frac{p}{2+p}} < u_{\rm P} = p\nu/\sqrt{3} \quad \Rightarrow \quad \nu > \sqrt{\frac{3}{p(2+p)}},$$
 (24c)

where the second case leads to a tracking constant attractor quintessence solution  $T \to P$  that is a straight line in the state space  $(\bar{\varphi}, u, v)$  with  $u = u_T = \sqrt{p/(2+p)}$ ,  $v = v_T = u_T/p\nu = 1/\sqrt{3}$ , which yields  $1 + w_{\varphi} = u_{\rm T}^2 = p/(2+p) = {\rm const.}$  throughout the entire evolution of the solution with  $\Omega_{\varphi} \equiv 3v^2 \bar{\varphi}^2 = \bar{\varphi}^2$ . In contrast, the first (last) case results in a tracking freezing (thawing) quintessence attractor solution, but in all cases  $T \to P$  is the interior boundary of the thawing quintessence surface of solutions, UFL<sub>0</sub><sup> $\varphi_*$ </sup>. Appropriate p and  $\nu$  yield viable tracking quintessence attractor solutions and thereby also viable thawing quintessence solutions, see Figure 3.

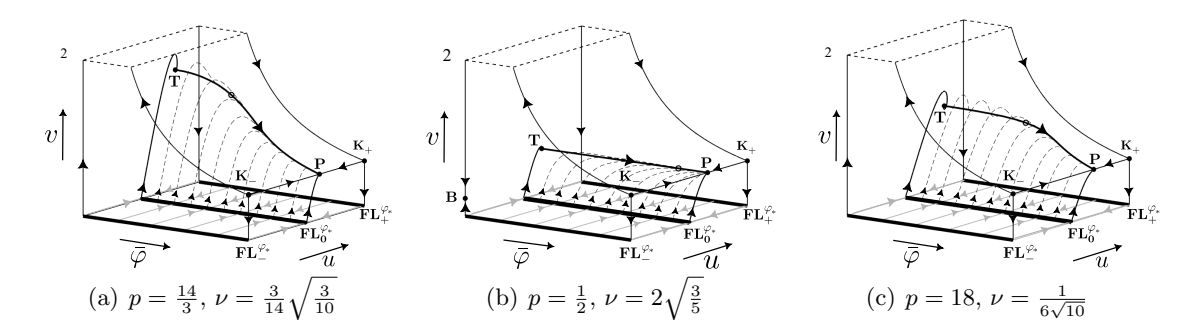


Figure 3: Illustration of the three cases of tracking quintessence attractor solutions with (a)  $w_{\varphi}|_{\rm T} = -0.7 \rightarrow w_{\varphi}|_{\rm P} = -0.9$ , (b)  $w_{\varphi} = w_{\varphi}|_{\rm T} = w_{\varphi}|_{\rm P} = -0.8$ , (c)  $w_{\varphi}|_{\rm T} = -0.9 \rightarrow w_{\varphi}|_{\rm P} = -0.8$ -0.7, for  $V = V_* \sinh^{-p}(\nu\varphi)$  (the ring denotes when  $\Omega_{\varphi} = 0.68$  for these solutions), and how they form the interior boundary of the thawing quintessence attractor solutions.

Next we consider the inverse power-law potential (Case I) and a generalisation of  $V \propto$  $\exp(M/\varphi) - 1$  (Case II):

$$V = V_* \varphi^{-p},$$
  $p > 0,$   $\lambda = \frac{p}{\varphi},$  (25a)

$$V = V_* \left[ \exp\left(\frac{p}{r}\varphi^{-r}\right) - 1 \right], \qquad p > 0, \quad r > 0, \qquad \lambda = \frac{p\varphi^{-(1+r)}}{1 - \exp\left(-\frac{p}{r}\varphi^{-r}\right)}. \tag{25b}$$

We choose

$$\bar{\varphi} \equiv \frac{\varphi^{\frac{1}{m}}}{1 + \varphi^{\frac{1}{m}}}, \qquad \varphi = \left(\frac{\bar{\varphi}}{1 - \bar{\varphi}}\right)^m, \quad \text{with} \quad m = 1 \quad \text{in Case I.}$$
 (26)

Choosing k = 1 + r in the definition of v in (21), with r = 0 in Case I, leads to

$$\bar{\varphi}' = 3\bar{\varphi}\,\tilde{G}(\bar{\varphi})\,uv,$$
 (27a)

$$u' = \frac{3}{2}(2 - u^2)(v H(\bar{\varphi}) - u), \tag{27b}$$

$$v' = \frac{3}{2} \left[ (1 - u^2)(1 - 3v^2 \bar{\varphi}^{2(1+r)m}) - 2(1+r)m \,\tilde{G}(\bar{\varphi}) \,uv \right] v, \tag{27c}$$

where

Case I: 
$$\tilde{G} = (1 - \bar{\varphi})^2$$
,  $H = p(1 - \bar{\varphi})$ ,  $r = 0$ , (28a)

Case I: 
$$\tilde{G} = (1 - \bar{\varphi})^2$$
,  $H = p(1 - \bar{\varphi})$ ,  $r = 0$ , (28a)  
Case II:  $\tilde{G} = \frac{1}{m} \bar{\varphi}^{rm} (1 - \bar{\varphi})^{1+m}$ ,  $H = \frac{p(1 - \bar{\varphi})^{(1+m)r}}{1 - \exp\left[-\frac{p}{r}\left(\frac{1 - \bar{\varphi}}{\bar{\varphi}}\right)^{rm}\right]}$ ,  $r > 0$ . (28b)

This dynamical system is regular for Case I, for which r = 0, m = 1, with T located at  $(\bar{\varphi}, u, v) = (0, \sqrt{p/(2+p)}, 1/\sqrt{p(2+p)}) \Rightarrow w_{\varphi} = -2/(2+p)$ . The system is also regular in

<sup>&</sup>lt;sup>5</sup>This solution was found by Sahni and Starobinsky (2000) [10] and Urena-Lopez and Matos (2000) [11].

Case II when r is a rational number and m is chosen as its denominator; for irrational values of r one can obtain arbitrary differentiability by choosing m sufficiently large. In Case II T is located at  $(\bar{\varphi}, u, v) = (0, 1, 1/p) \Rightarrow w_{\varphi} = 0$ . This might tempt one to conclude that the tracking quintessence solution is a scaling freezing quintessence solution, but this is not the case since  $\lim_{N\to-\infty} \rho_{\varphi}/\rho_{\rm m} = 0$  and not a positive constant as it was for scaling freezing quintessence. This is due to that the tracking quintessence solution now is the unstable *centre* manifold of T corresponding to an eigenvalue that is zero. The (stronger) attracting properties of this solution is thereby more like the inflationary attractor solutions than the previous scaling freezing and tracking quintessence models, which corresponded to an unstable manifold associated with a positive eigenvalue, illustrated in Figures 2(b) and 3, respectively. One example of each of the present cases is given in Figure 4, showing that the tracking quintessence attractor solution is the interior boundary of the thawing quintessence UFL $_0^{\varphi_*}$  surface of solutions.

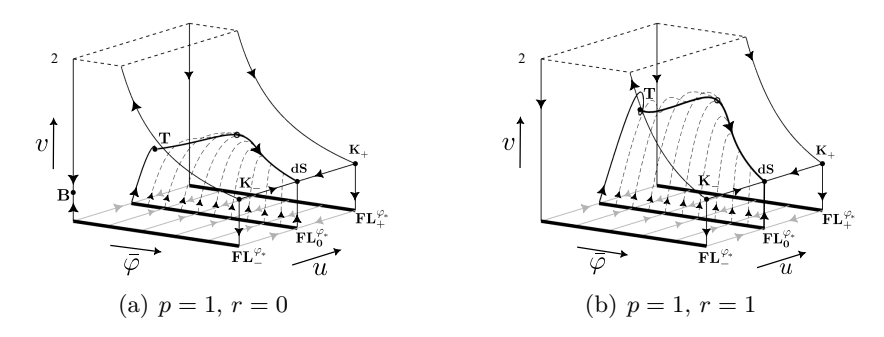


Figure 4: The figures depict the tracking attractor quintessence solution  $T \to dS$  (the ring denotes when  $\Omega_{\varphi} = 0.68$ ), showing that it is the interior boundary of the surface of thawing quintessence solutions. The  $FL_0^{\varphi_*} \to T$  solution on the boundary  $\bar{\varphi} = 0$  illustrates that the tracker fixed point T is a stable focus on this boundary; (a) shows the key quintessence aspects for  $V \propto \varphi^{-p}$  whereas (b) depicts them for  $V \propto \exp(\frac{p}{r}\varphi^{-r}) - 1$ . Note that the tracking quintessence solution  $T \to dS$  in (b) is the unstable *centre* manifold of T.

### 4 Quintessence approximations

In [12] (AU) new approximations were introduced for thawing quintessence and for tracking quintessence with asymptotic inverse power-law potentials. These approximations are simpler and more accurate than any previous ones in the literature, as shown in [12, 13]. They are based on the DE assumptions: (i)  $\lim_{N\to-\infty} w_{\rm DE} = w_{\infty}$ ,  $w_{\infty} \in [-1,0)$ ; (ii) past asymptotic matter-domination,  $\lim_{N\to-\infty} \Omega_{\rm m} = 1$ ,  $\lim_{N\to-\infty} \Omega_{\rm DE} = 0$ . The field equations for matter consisting of  $\rho_{\rm m}$  and  $\rho_{\rm DE}$  then results in corrections by coupled series expansions in

$$T = T_0 e^{-3w_\infty N},\tag{29}$$

for  $w_{\rm DE}$  and  $\Omega_{\rm DE}$  given by

$$w_{\rm DE} = w_{\infty} \left[ 1 - \alpha T + \alpha \beta T^2 + \dots \right], \tag{30a}$$

$$\Omega_{\rm DE} = T \left( 1 - (1 + \alpha)T + \left[ 1 + \frac{1}{2}\alpha \left( 4 + \alpha + \beta \right) \right] T^2 + \dots \right).$$
(30b)

The following Padé approximant for  $w_{\rm DE}$  is then constructed from (30a),

$$w_{\rm DE} = [1/1]_{w_{\rm DE}}(T) = w_{\infty} \left( 1 - \frac{\alpha T}{1 + \beta T} \right) \quad \Rightarrow \quad w_{\rm DE}' = \frac{3w_{\infty}^2 \alpha T}{(1 + \beta T)^2}.$$
 (31)

Setting  $\alpha = 0$  leads to models with  $w_{\rm DE} = w_{\infty}$  and thereby the  $\Lambda {\rm CDM}$  model when  $w_{\infty} = -1$ . If one is so inclined, it is possible to solve for  $\alpha$  and  $\beta$  in terms of  $w_{\rm DE0}$  and  $w'_{\rm DE0}$  at a reference time  $t_0 \Rightarrow N = \ln(a/a_0) = 0$  (subscripts  $_0$  refer to the reference time  $t_0$ ), which leads to

$$w_{\rm DE} - w_{\infty} = \frac{3w_{\infty}(w_{\rm DE0} - w_{\infty})}{3w_{\infty} + \xi_0(1 - \exp(3w_{\infty}N))}, \qquad \xi \equiv \frac{(w_{\rm DE} - w_{\infty})'}{w_{\rm DE} - w_{\infty}},$$
 (32)

where  $T_0$  drops out from the calculation (cf. with [13] for the thawing case  $w_{\infty} = -1$ ). Note that although the parameter  $w_{\rm DE}(N)$  is not an observable quantity, it can, however, together with  $\rho_{\rm m} \propto \exp(-3N)$ , be used to compute observables such as the Hubble variable, see AU.

The importance of the DE results is that they yield simple and accurate approximations for thawing quintessence ( $w_{\infty} = -1$ ) and tracking quintessence for asymptotically inverse power-law potentials, for which  $w_{\infty} \in (-1,0)$ , where  $w_{\text{DE}}$  in (31) is replaced with

$$w_{\varphi} \approx w_{\infty} \left( 1 - \frac{\alpha T}{1 + \beta T} \right).$$
 (33)

However, setting  $\alpha$  and  $\beta$ , or, equivalently,  $w_{\varphi 0}$  and  $w'_{\varphi 0}$ , to optimize quintessence approximations only amounts to curve fitting, see [13]. To obtain non-numerical predictive power, equation (30b) was used in AU to construct  $\Omega_{\varphi} \approx [1/1]_{\Omega_{\varphi}}(T) = \frac{T}{1+(\alpha+1)T}$ , which results in<sup>7</sup>

$$T_0 = \frac{\Omega_{\varphi 0}}{\Omega_{m0} - \alpha \Omega_{\varphi 0}} \qquad (\Omega_{m0} + \Omega_{\varphi 0} = 1)$$
(34)

and thereby

$$w_{\varphi} \approx [1/1]_{w_{\varphi}}(T) = w_{\infty} \left( 1 - \frac{\alpha \Omega_{\varphi 0}}{\beta \Omega_{\varphi 0} + (\Omega_{m0} - \alpha \Omega_{\varphi 0})e^{3w_{\infty}N}} \right). \tag{35}$$

As shown in AU, for thawing quintessence the field equations yield

$$\alpha = \left(\frac{2}{3}\right)^3 \epsilon_*, \qquad \beta = \frac{3}{5} - \left(\frac{2}{3}\right)^3 \epsilon_* + \frac{4}{15}\eta_*,$$
 (36)

where  $\epsilon_*$  and  $\eta_*$  are the slow-roll parameters

$$\epsilon(\varphi) \equiv \frac{1}{2} \left( \frac{V_{,\varphi}}{V} \right)^2 = \frac{\lambda^2}{2}, \qquad \eta(\varphi) \equiv \frac{V_{,\varphi\varphi}}{V} = \lambda^2 - \lambda_{,\varphi},$$
 (37)

computed at  $\varphi = \varphi_*$  on  $\mathrm{FL}_0^{\varphi_*}$  and thereby the frozen value  $\varphi = \varphi_*(\bar{\varphi}_*)$  on the matter-dominated boundary v = 0. Tracking quintessence for asymptotic inverse power-law potentials yields more complicated expressions involving

$$\Gamma = \frac{V V_{,\varphi\varphi}}{V_{\varphi}^2} = 1 + (\lambda^{-1})_{,\varphi}; \tag{38}$$

the parameters  $\alpha$  and  $\beta$  are given by

$$\alpha = -w_{\infty}^{-1}(1 - w_{\infty}^2)k,\tag{39a}$$

$$\beta = \frac{2w_{\infty}^2(3w_{\infty} - 1) + k\left(12w_{\infty}^4 - w_{\infty}^3 - 3w_{\infty}^2 + 2w_{\infty} - 1\right) + k^{(2)}}{w_{\infty}(12w_{\infty}^2 - 3w_{\infty} + 1)},$$
(39b)

$$k = \frac{w_{\infty} - \frac{2}{3}\Gamma^{(1)}}{4w_{\infty}^2 - 2w_{\infty} + 1}, \qquad k^{(2)} = \frac{w_{\infty}\Gamma^{(2)}}{9(w_{\infty} + 1)k}, \tag{39c}$$

<sup>&</sup>lt;sup>6</sup>When  $t_0$  refers to the present time it is easy to express results in the redshift z since then  $\exp(-N) = 1 + z$ .

<sup>7</sup>In AU  $\gamma = 1 + \alpha$  was used instead of  $\alpha$  since this leads to the simpler expression  $T_0 = \Omega_{\varphi 0}/(1 - \gamma \Omega_{\varphi 0})$ .

5 DISCUSSION 11

where

$$\Gamma(\tilde{\varphi}) \approx \Gamma^{(0)} + \Gamma^{(1)}\tilde{\varphi} + \frac{1}{2}\Gamma^{(2)}\tilde{\varphi}^2 + \dots, \qquad \Gamma^{(n)} = \left. \frac{d^n \Gamma}{d\tilde{\varphi}^n} \right|_{\tilde{\varphi} = 0}, \qquad \Gamma^{(0)} = 1 + p^{-1}, \qquad (40)$$

and  $\tilde{\varphi} \equiv \lambda^{-2}(\varphi)$ . Note that for  $V \propto \varphi^{-p}$  it follows that  $\Gamma = 1 + p^{-1} = \text{const.}$  and  $w_{\infty} = p/(2+p)$ , which makes the above expressions collapse to relatively simple expressions.

### 5 Discussion

The methods and results in this paper are easy to generalise, for both various DE models and potentials. For example, the potential  $V = V_* \left[ \exp \left( \frac{p}{r} \varphi^{-r} \right) - 1 \right]$  belongs to a much larger class of potentials that is straightforward to treat with the present ideas and techniques:

$$V = V_* \exp[pf^{-r}(\varphi)/r], \qquad V = V_* \left(\exp[pf^{-r}(\varphi)/r] - 1\right); \qquad V_* > 0, \quad r > 0, \tag{41}$$

where  $\lim_{\varphi \to 0} [\varphi^{-1} f(\varphi)] = 1$ , exemplified by (cf. eq. (19)):

$$f = \frac{\sinh(\nu\varphi)}{\nu \cosh^{1-\alpha}(\nu\varphi)} = \frac{\tanh(\nu\varphi)}{\nu[1 - \tanh^2(\nu\varphi)]^{\alpha/2}}.$$
 (42)

Choosing u and v as in Section 3 and

$$\bar{\varphi} = \tanh^{\frac{1}{m}}(\nu\varphi) \in [0, 1], \qquad m > 0, \quad \nu > 0, \tag{43}$$

yields dynamical systems problems resembling those in the previous section.

We have only considered monotonically decreasing potentials, but there are also, e.g., potentials with positive minima that are cosmologically interesting, and with new features. For example, a potential with two exponential terms, as in (15), with  $\lambda_- > \sqrt{6}$  and  $\lambda_+ < -\sqrt{6}$  yields a potential with a positive minimum and a past attractor that is not a fixed point but a so-called heteroclinic cycle, see AUW1 for further details. Thus, local fixed point analysis does not always suffice for a description of asymptotics and global structure, even for quite simple models. In this context, it was only recently that models with an exponential potential and matter with a linear equation of state were analysed globally [14], using the synergy between Hamiltonian and dynamical systems formulations to derive monotonic functions, which are crucial for global results. Initially these models were analysed by using  $\Sigma_{\varphi} = \varphi'/\sqrt{6}$  and  $\sqrt{\Omega_{\varphi}}$  as variables, which subsequently in the literature have been used for a variety of more general potentials, even though they often are quite inappropriate, illustrating that some variables needlessly result in nonregular equations or/and state space coordinate singularities leading to unphysical fixed points, or sets of fixed points with overly many eigenvalues with zero real parts.

Models with matter and a potential with zero minima or a minimum provide other interesting examples, as illustrated by monomial potentials. For these models it is better to use other variables than  $(\bar{\varphi}, \Sigma_{\varphi}, \sqrt{\Omega_{\varphi}})$  or  $(\bar{\varphi}, u, v)$ , such as those in [15, 16], which result in that the matter-dominated subset is described by an isolated FL fixed point. In this case the one-parameter subset of thawing quintessence solutions corresponds to the unstable manifold of FL with two positive eigenvalues while the stable subset, associated with a single negative eigenvalue, pushes an open subset of solutions to this thawing attractor quintessence solution subset. Note also that apart from the thawing quintessence attractor solutions these models also admit two (equivalent) inflationary attractor solutions. Furthermore, in [16] a new dynamical systems averaging method was introduced to deal with the future asymptotics, which for some of these models consist of periodic solution trajectories.

Even though two different dynamical systems formulations both yield regular and bounded state spaces, one of these might still be preferable. For example, consider the asymptotically REFERENCES 12

inverse power-law potential problem for which we regularised the equations by changing the definition of v from  $v = \sqrt{\Omega_{\varphi}/3}$  to  $v = \bar{\varphi}^{-1}\sqrt{\Omega_{\varphi}/3}$ . If we instead of changing v choose a new time variable  $\tilde{\tau}$  defined by  $d\tilde{\tau}/dN \equiv \bar{\varphi}^{-1}$  this also regularises the equations. This, however, results in structures on the  $\bar{\varphi} = 0$  boundary that prevent asymptotic analytic results and an identification of the past asymptotic state of the tracking quintessence attractor solution.

Another example was given in AUW1 where two state space formulations were used to deal with potentials with bounded  $\lambda$ :  $(\bar{\varphi}, \Sigma_{\varphi}, \Omega_{\rm m})$  and  $(\bar{\varphi}, u, v)$ . Both yield regular equations and bounded state spaces. The first formulation, however, collapses the matter-dominated boundary v = 0 to a line of fixed points, which hides the evolution of  $w_{\varphi}$  during the matter-dominated epoch, easily seen in u, where  $w_{\varphi}(N)$  is often plotted in graphs in papers about quintessence.

Although having a global state space picture has several advantages, apart from the most simple problems there typically are different physical and mathematical structures at different parts of the state space. It is therefore often advantageous to cover different parts of the state space with different variables adapted to the local structures, e.g., the approximations in Section 4 were based on locally useful unbounded scalar field variables adapted to the past asymptotic features of the thawing and tracking quintessence attractor solutions.

In conclusion, a thorough understanding of a model, using dynamical systems reformulations of the field equations as a powerful tool, requires variables that are adapted to the physical and mathematical structures of the problem at hand.

Finally, note that some of the presently cited papers contain brief descriptions of the historical developments concerning dynamical systems in cosmology with a focus on scalar field cosmology. As described in [15], this history begins in the mid 1980s with inflationary models with potentials with zero minima. This was later followed by models with an exponential potential, as described in [14], but note also the book [17] by A. Coley. See [4] and [8] for historical backgrounds on quintessential inflation and tracking quintessence, respectively. In addition, see the introductory survey by S. Cotsakis and A. Yefremov in this volume.

#### Acknowledgments

A. A. is supported by FCT/Portugal through FCT/Tenure 2023.15700. TENURE.003/CP00055/CT00003, CAMGSD, IST-ID, grant No. UID/4459/2025, and projects 2024.04456.CERN, and H2020-MSCA-2022-SE EinsteinWaves, GA No. 101131233. A. A. would also like to thank the CMA-UBI in Covilhã for kind hospitality. C. U. would like to thank the CAMGSD, Instituto Superior Técnico in Lisbon for kind hospitality and, finally, John Wainwright for friendship and several decades of collaboration, including on quintessence.

### References

- [1] R. R. Caldwell and E. V. Linder. Limits of quintessence. Phys. Rev. Lett., 95:141301, 2005.
- [2] A. Alho, C. Uggla, and J. Wainwright. Quintessence from a state space perspective. *Physics of the Dark Universe*, **39**:101146, 2023.
- [3] K. Dimopoulos and C. Owen. Quintessential inflation with  $\alpha$ -attractors. J. of Cosmology and Astroparticle Physics, **06**:027, 2017.
- [4] A. Alho and C. Uggla. Quintessential  $\alpha$ -attractor inflation: A dynamical systems analysis. Journal of Cosmology and Astroparticle Physics, 11:083, 2023.
- [5] Y. Akrami et al. Dark energy,  $\alpha$ -attractors, and large-scale structure surveys. JCAP, **06**:041, 2018.

REFERENCES 13

[6] P. J. Steinhardt, L. Wang, and I. Zlatev. Cosmological tracking solutions. Phys. Rev. D, 59:123504, 1999.

- [7] I. Zlatev, L. Wang, and P. J. Steinhardt. Quintessence, cosmic coincidence and the cosmological constant. *Phys. Rev. Lett.*, **82**:896, 1999.
- [8] A. Alho, C. Uggla, and J. Wainwright. Tracking quintessence. *Physics of the Dark Universe*, 44:101433, 2024.
- [9] S. Tsujikawa. Quintessence: a review. Class. Quantum Grav., 30:214003, 2013.
- [10] V. Sahni and A.Starobinsky. The case for a positive cosmological lambda-term. Int. J. Mod. Phys. D, 9:373, 2000.
- [11] L.A. Urena-Lopez and T. Matos. New cosmological tracker solution for quintessence. *Phys. Rev. D*, **62**:081302, 2000.
- [12] Artur Alho and Claes Uggla. New simple and accurate quintessence approximations. Phys. Rev. D, 111:083549, Apr 2025.
- [13] David Shlivko, Paul J. Steinhardt, and Charles L. Steinhardt. Optimal parameterizations for observational constraints on thawing dark energy. *Journal of Cosmology and Astroparticle Physics*, 2025(06):054, jun 2025.
- [14] A. Alho, W. C. Lim, and C. Uggla. Cosmological global dynamical systems analysis. *Class. Quantum Grav.*, **39**:145010, 2022.
- [15] A. Alho and C. Uggla. Global dynamics and inflationary center manifold and slow-roll approximants. *Journal of Mathematical Physics*, **56**(012502), 2015.
- [16] A. Alho, J. Hell, and C. Uggla. Global dynamics and asymptotics for monomial scalar field potentials and perfect fluids. *Class. Quant. Grav.*, **32**(14):145005, 2015.
- [17] A. A. Coley. *Dynamical systems and cosmology*. Kluwer Academic Publishers, Dordrecht, 2003.